

# Radiation Pattern of Waveguide Antenna Arrays on Spherical Surface - Experimental Results

Slavko Rupčić, Vanja Mandrić, Davor Vinko

J.J.Strossmayer University of Osijek, Faculty of Electrical Engineering, Osijek, Croatia  
slavko.rupcic@etfos.hr, vanja.mandric@etfos.hr, davor.vinko@etfos.hr

**Abstract** – In this paper, the radiation pattern of two experimental models of circular waveguide antenna arrays on spherical surface is obtained experimentally and compared with theoretical patterns. We have omitted the phase delay of feed system signals because we have only compared measured and theoretical results in order to verify theoretical results, without trying to improve the best radiation characteristics of developed experimental models. Analysis was made with a developed moment method (MoM) program. The spectral-domain approach to the analysis of the spherical antenna arrays is briefly presented in the paper. Measurements were not performed in a well-defined anechoic environment.

**Keywords** – radiation pattern, differential radiation pattern, antenna array, spherical array, waveguide

## 1. INTRODUCTION

An array of antennas disposed on the surface of a sphere is of importance because such an array provides wide hemispherical scan coverage with low grating lobe levels. Spherical array antennas combine the capabilities of array antennas with the optimal geometry to achieve omni-directional coverage.

Thus, spherical arrays are an attractive solution and an optimal choice for satellite tracking, telemetry and command applications.

At the present time little information is available on the radiation characteristics of spherical antenna arrays.

The array was modeled using a previously presented computer program based on the method of moments in spectral domain [8].

In the process of verifying theoretical results we built two experimental models and validated theoretical results by comparing the results to the measurements performed on the developed laboratory models.

We also discuss the results of an experimental investigation of two spherical arrays consisting of circular waveguide elements with apertures on a hemispherical ground plane.

## 2. FAR FIELD CALCULATION

Conformal antennas and periodic structures are frequently analyzed by means of the electric field integral equation and the moment method. The kernel of the integral operator is Green's function, which is different for different structures.

An electrical field radiated by the current shell on the spherical surface in homogeneous media is:

$$\mathbf{E}(r, \theta, \varphi) = \sum_{m=-\infty}^{\infty} \sum_{n=|m|}^{\infty} \bar{\mathbf{L}}(n, m, \theta) \cdot \bar{\mathbf{G}}(n, m, r | r_s) \tilde{\mathbf{M}}(r, n, m) e^{jm\varphi} \quad (1)$$

where  $\bar{\mathbf{G}}(n, m, r | r_s)$  is a spectral domain dyadic Green's function for a grounded spherical surface and  $\bar{\mathbf{L}}(n, m, \theta)$  is the kernel of the vector-Legendre transformation.  $\tilde{\mathbf{M}}(r, n, m)$  is a spectral domain equivalent magnetic current placed at the open of each waveguide [5], [6].

The appropriate spectral-domain Green's function of a multilayer spherical structure is calculated using the G1DMULT algorithm [1], [2].

The radiation pattern of the array is obtained as a superposition of fields excited by each waveguide aperture (placed on a spherical surface at the point with coordinate  $(\alpha_n, \beta_n)$ ):

$$E_{\theta, \alpha_n, \beta_n}(\theta, \phi) = -\frac{\cos \theta \sin \alpha_n \cos(\phi - \beta_n) - \sin \theta \cos \alpha_n}{\sin \theta} E_{\theta}(\theta', \phi') - \frac{\sin \alpha_n \sin(\phi - \beta_n)}{\sin \theta} E_{\phi}(\theta', \phi') \quad (2)$$

$$E_{\varphi, \alpha_n, \beta_n}(\theta, \varphi) = \frac{\sin \alpha_n \sin(\varphi - \beta_n)}{\sin \theta} E_{\theta}(\theta', \varphi') - \frac{\cos \theta \sin \alpha_n \cos(\varphi - \beta_n) - \sin \theta \cos \alpha_n}{\sin \theta} E_{\varphi}(\theta', \varphi') \quad (3)$$

where  $\alpha_n$  and  $\beta_n$  are the  $\theta$  and  $\phi$  coordinate of each antenna element in the global coordinate system [3], [4].

We introduced local coordinate systems with the origin located at the center of each antenna element (shown in Fig.1).

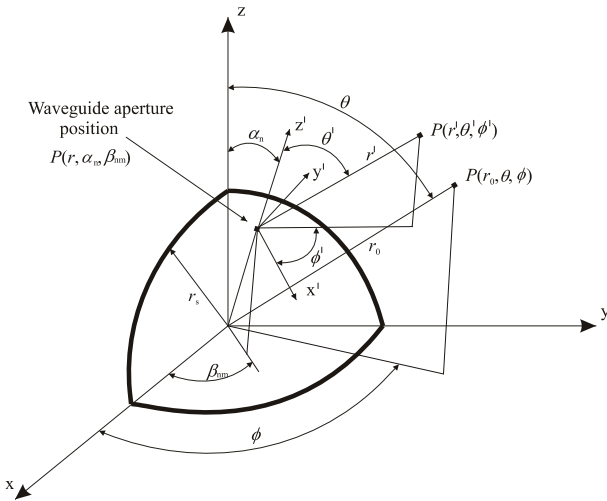


**Fig. 1.** Global and local coordinate system.



**Fig. 2.** Spherical experimental model (MODEL I) with two waveguides ( $\alpha_1=0^\circ, \beta_{11}=0^\circ, \alpha_2=18^\circ, \beta_{21}=90^\circ$ ).

The complete pattern expression of the field produced by the array is given as:

$$\mathbf{E}(\theta, \varphi) = \sum_{n,m} \mathbf{E}_{\alpha_n \beta_{nm}}(\theta, \varphi) \quad (3)$$

### 3. EXPERIMENTAL MODELS OF A SPHERICAL ARRAY

The considered antennas are designed with circular waveguides used as antenna elements placed on the spherical structure. The antenna elements are placed at equidistant position on the (grounded) surface of the icosahedron.

The first array (MODEL I – shown in Fig. 2.) design specifications are:

- first waveguide position:  $\alpha_1=0, \beta_{11}=0$ ;
- second waveguide position:  $\alpha_2=18^\circ, \beta_{21}=90^\circ$ ;
- radii:  $r_s=69$  cm and  $r_w=6$  cm.

The second array (MODEL II – shown in Fig. 3.) design specifications are:

- first waveguide position:  $\alpha_1=0, \beta_{11}=0$ ;
- second ring waveguide position:  $\alpha_2=56^\circ, \beta_{21}=36^\circ, \beta_{22}=108^\circ, \beta_{23}=180^\circ, \beta_{24}=252^\circ, \beta_{25}=324^\circ$ ;
- radii:  $r_s=30$  cm and  $r_w=6$  cm.

Further, normalized free-space radiation patterns were calculated and measured at the frequency  $f = 1.75$  GHz.



**Fig. 3.** Spherical experimental model (MODEL II) with six waveguides ( $\alpha_1=0^\circ, \beta_{11}=0^\circ, \alpha_2=56^\circ, \beta_{21}=36^\circ, \beta_{22}=108^\circ, \beta_{23}=180^\circ, \beta_{24}=252^\circ, \beta_{25}=324^\circ$ ).

### 4. THEORETICAL AND MEASURED RESULTS

Consider an antenna arrays transmitting a wave into the far field region where strength of its field is to be measured. All the array elements (waveguides) are excited in same phase with uniform amplitude. The antenna arrays were oriented in a fixed position and both E- and H- plane patterns have been recorded. The radiation patterns produced by two experimental models were measured over the azimuthal angle ranging from  $-90^\circ$  to  $90^\circ$ .

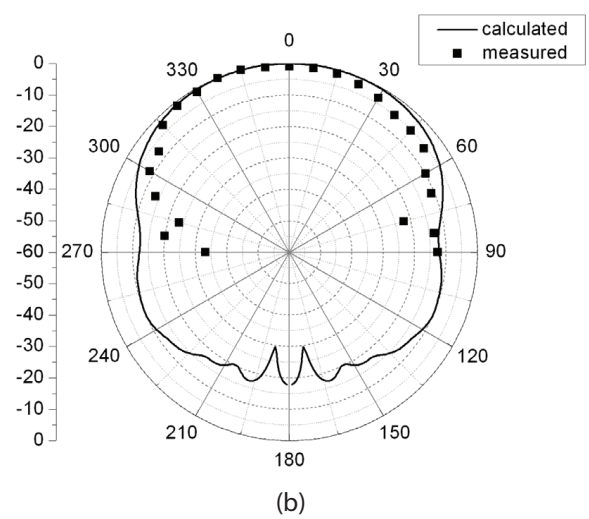
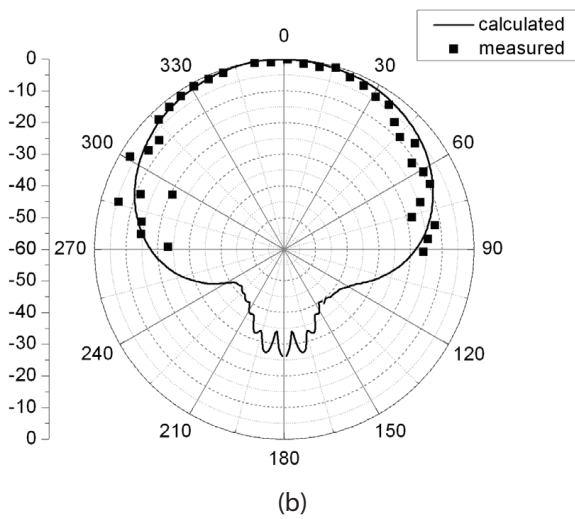
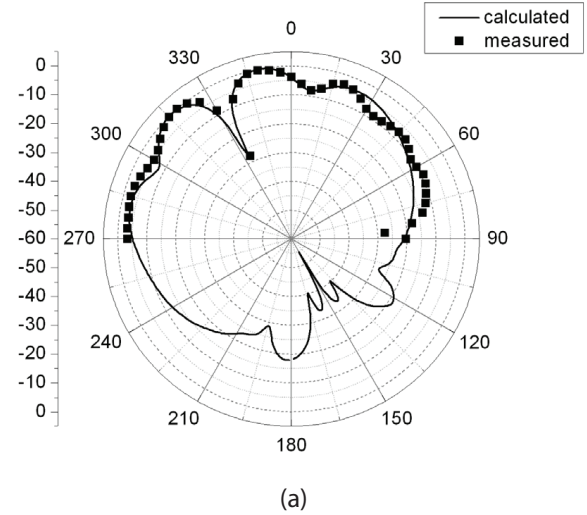
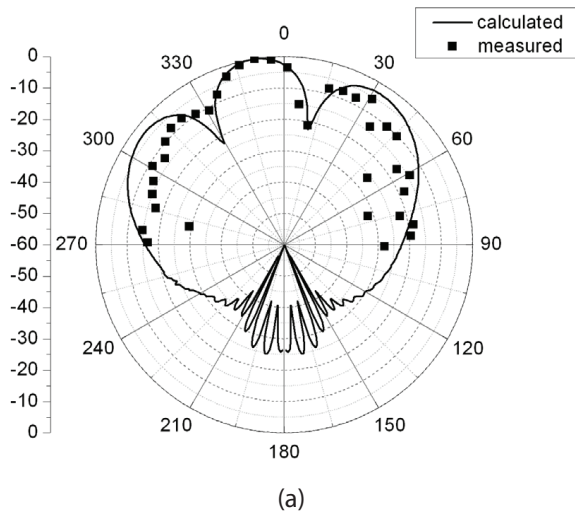


**Fig. 4.** Normalized radiation pattern of two waveguide - fed aperture arrays on a spherical surface – MODEL I:  
a) H - plane;  
b) E - plane; ( $\alpha_1=0^\circ, \beta_{11}=0^\circ, \alpha_2=18^\circ, \beta_{21}=90^\circ$ ) [8].

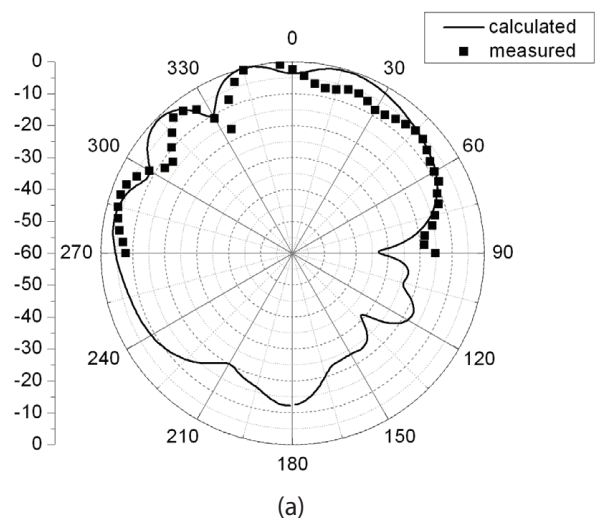
**Fig. 5.** Normalized differential radiation pattern of two waveguide - fed aperture arrays on a spherical surface – MODEL II:  
a) E - plane;  
b) H - plane. ( $\alpha_1=0^\circ, \beta_{11}=0^\circ, \alpha_2=56^\circ, \beta_{21}=180^\circ$ ) [7].

As expected, the main beam peak of the radiation pattern is on a half value of the second waveguide position angle  $\theta_{np} = \frac{\alpha_2}{2} = 9^\circ$  (or precisely  $-9^\circ$ ).

Theoretical and measured free-space normalized radiation patterns of two waveguide antennas (MODEL I) on the spherical surface are shown in Fig. 4.

Figures 5., 6. and 7. show free-space normalized radiation patterns of antenna arrays (MODEL II) with a different number of elements (waveguides) which are activated (two, three and six waveguides, respectively).

As can be seen in Figure 5., the notch-peak of the differential radiation pattern is on a half value of the second waveguide position angle  $\theta_{np} = \frac{\alpha_2}{2} = 28^\circ$  (or precisely  $-28^\circ$ ).



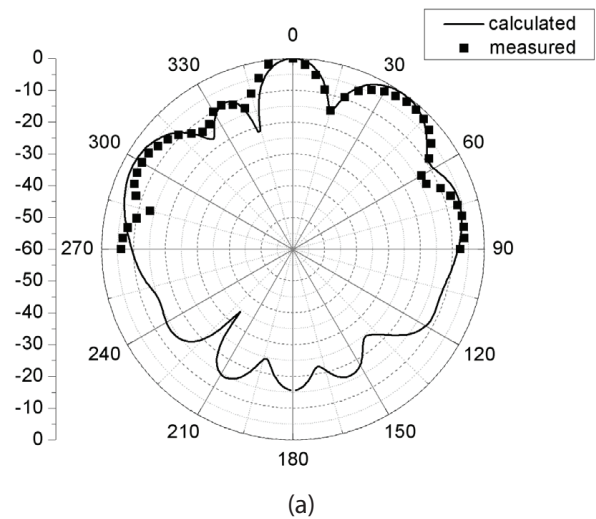
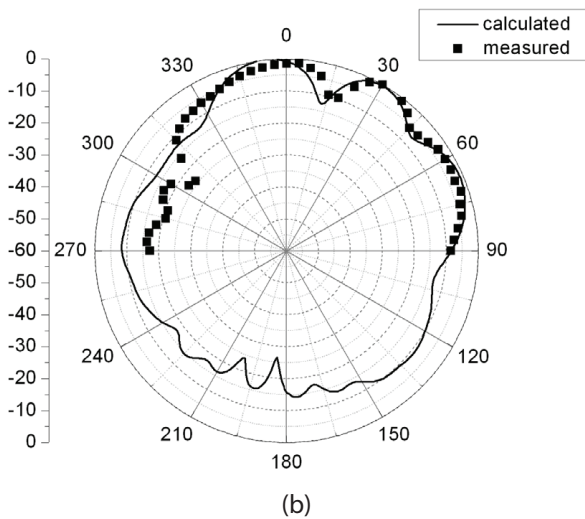


**Fig. 6.** Radiation pattern of a spherical array consisting of three waveguide-fed aperture arrays on a spherical surface – MODEL II:

a) E - plane;

b) H – plane (excited waveguides on positions:  $\alpha_1=0^\circ$ ,  $\beta_{11}=0^\circ$ ,  $\alpha_2=56^\circ$ ,  $\beta_{21}=108^\circ$ ,  $\beta_{22}=180^\circ$ ) [8].

Moreover, we achieve a very good agreement between the theoretical and the measured normalized radiation pattern regarding the main beam and side lobes. What has to be mentioned here is that the grating lobe amplitude is lower than the main beam but not enough. The reason is that the antenna elements are not phased such that the pattern produced by an array has maximum along the direction  $\theta_{max}$  and  $\varphi_{max}$  and the inter-element distances are not optimal.

Prior to the statistical analysis the measurement interval ( $-90 \leq \theta \leq 90$ ) is dissected into two intervals:

1. **main beam (notch-peak) interval:** maximum radiation direction angle (main beam)  $\pm 30^\circ$  (Figures 4., 6., and 7.) and notch peak angle  $\pm 30^\circ$  (Fig. 5.);
2. **other interval:** outside of the main beam interval.

Tables 1, 2, 3 and 4 show descriptive statistics for the average difference of theoretical and measured results. As can be seen, the maximal absolute average difference in the main beam intervals ranges between 0.65 and 1.99 dB, except for Fig.6a where the difference is 3.81 dB. The average difference in other intervals ranges between 2.0 and 7.0 dB.

The results indicate that the amount of errors (measurement errors, method errors and laboratory model errors), defined as the absolute difference of theoretical and measured results and analyzed by statistic parameters, does not have important effects on radiation of these spherical arrays. Furthermore, the measured results suggest that the developed theoretical model and computer program are performed very well.

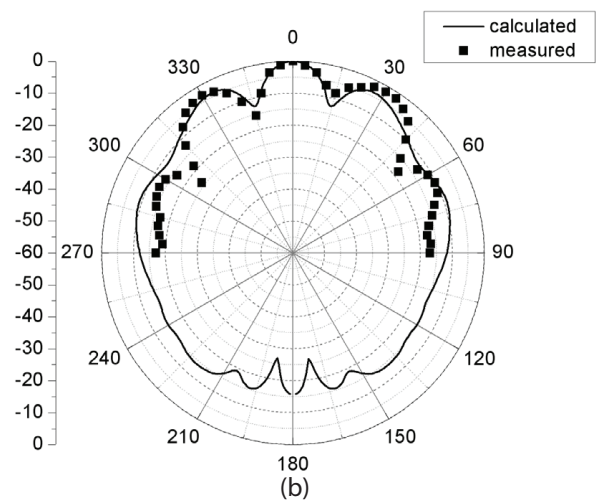


**Fig. 7.** Radiation pattern of six waveguide-fed aperture arrays on a spherical surface – MODEL II:

a) E - plane;

b) H – plane ( $\alpha_1=0^\circ$ ,  $\beta_{11}=0^\circ$ ,  $\alpha_2=56^\circ$ ,  $\beta_{21}=36^\circ$ ,  $\beta_{22}=108^\circ$ ,  $\beta_{23}=180^\circ$ ,  $\beta_{24}=252^\circ$ ,  $\beta_{25}=324^\circ$ ).

## 5. CONCLUSION

In this paper, we have shown the radiation pattern of two spherical antenna arrays. Analysis of the arrays was made with the developed moment method program.

The results obtained from the theoretical investigation are verified by comparison with measured results.

The errors in the measured results appear due to experimental model errors, diffraction from the edges of the semi-spherical surface and reflections inside the measurement room which is not a well-defined anechoic chamber.

Descriptive statistic parameters confirmed a very good agreement between theoretical and measured normalized radiation patterns.



## REFERENCES

- [1] P.-S. Kildal and J. Sanford, "Analysis of conformal antennas by using spectral domain techniques for curved structures," *Proceedings of COST 245 - ESA workshop on active antennas*, Noordwijk, pp. 17-26, 1996.
- [2] Z. Sipus, P.-S. Kildal, R. Leijon and M. Johansson, "An algorithm for calculating Green's functions for planar, circular cylindrical and spherical multilayer substrates," *Applied Computational Electromagnetics Society Journal*, Vol. 13, pp. 243-254, 1998.
- [3] D. L. Sengupta, T. M. Smith and R. W. Larson, "Radiation Characteristics of Spherical Array of Circularly Polarized Elements," *IEEE Trans. on Antennas and Propagation*, Vol. 16, pp. 2-7, Jan. 1968.
- [4] D. L. Sengupta, J.E.Ferris and T. M. Smith, "Experimental Study of a Spherical Array of Circularly Polarized Elements", *Proceedings of the IEEE*, pp. 2048-2051, Nov. 1968.
- [5] Z. Sipus, S. Rupcic, M. Lanne and L. Josefsson, "Analysis of Circular and Spherical Array of Waveguide Elements Covered with Radome", *Proceedings of IEEE International Symposium on Antennas and Propagation*, Boston, USA, pp. II 350-353, 2001.
- [6] N. Burum, S. Rupcic and Z. Sipus, "Theoretical and Experimental Study of Spherical Arrays", *IEEE MELECON 2004, Dubrovnik*, Croatia, pp. II 503-506, 2004.
- [7] S. Rupcic and V. Mandric, "Effect of Experimental Model Errors on Radiation Pattern of a Spherical Aperture Antennas Array", *ELMAR 2008*, Zadar, Croatia, pp. 240 - 245, 2008.
- [8] S. Rupcic,, "Circular Waveguide Antenna Arrays on Spherical Structures", PhD Thesis, *University of Zagreb, Faculty of Electrical Engineering and Computing*, Zagreb, 2009.

**Tab. 1.** Descriptive statistics for the absolute difference of theoretical and measured results of a spherical array consisting of two waveguide-fed apertures – MODEL I.

Fig.4a)					
INTERVALS (deg)	MEAN (dB)	STD (dB)	MEDIAN (dB)	P25 (dB)	P75 (dB)
-90≤θ≤+90	5.14954	4.95528	4.11	1.34	7.39
-39≤θ≤+27	1.99663	2.36085	1.04	0.35	3.24
-90≤θ<-39 and +27<θ≤+90	7.0687	5.16822	6.16	3	8.79
Fig.4b)					
-90≤θ≤+90	2.29205	2.55099	1.41	0.51	3.18
-30≤θ≤+30	0.65217	0.45205	0.46	0.47	1.055
-90≤θ<-30 and +30<θ≤+90	3.0792	2.77085	2.14	1.96	4.34

**Tab. 2.** Descriptive statistics for the absolute difference of theoretical and measured results of a spherical array consisting of two waveguide-fed apertures – MODEL II.

Fig.5a)					
INTERVALS (deg)	MEAN (dB)	STD (dB)	MEDIAN (dB)	P25 (dB)	P75 (dB)
-90≤θ≤+90	1.81386	2.02812	0.97	0.4	2.27
-58≤θ≤+2	1.37337	2.49723	0.525	0.21	0.82
-90≤θ<-58 and +2<θ≤+90	2.02742	1.76143	1.55	0.82	3.11
Fig.5b)					
-90≤θ≤+90	4.16662	5.05019	2.97	0.91	4.47
-30≤θ≤+30	1.07933	0.94081	0.91	0.597	1.24
-90≤θ<-30 and +30<θ≤+90	5.90322	5.60351	4.08	1.7	6.7058

**Tab. 3.** Descriptive statistics for the absolute difference of theoretical and measured results of a spherical array consisting of three waveguide-fed apertures – MODEL II.

<b>Fig.6a)</b>					
<b>INTERVALS (deg)</b>	<b>MEAN (dB)</b>	<b>STD (dB)</b>	<b>MEDIAN (dB)</b>	<b>P25 (dB)</b>	<b>P75 (dB)</b>
-90≤θ≤+90	3.41388	3.48686	2.14	1.02	5.3
-58≤θ≤+2	3.81063	3.43463	2.12	1.1	5.94
-90≤θ<-58 and +2<θ≤+90	3.22152	3.54834	2.44	0.76	4.99
<b>Fig.6b)</b>					
-90≤θ≤+90	1.71	3.26349	1.71	0.99	5
-2≤θ≤+58	1.53875	1.60089	1.115	0.5	1.5
-90≤θ<-2 and +58<θ≤+90	4.16548	3.52857	2.33	1.42	6.88

**Tab. 4.** Descriptive statistics for the absolute difference of theoretical and measured results of a spherical array consisting of six waveguide-fed apertures – MODEL II.

<b>Fig.7a)</b>					
<b>INTERVALS (deg)</b>	<b>MEAN (dB)</b>	<b>STD (dB)</b>	<b>MEDIAN (dB)</b>	<b>P25 (dB)</b>	<b>P75 (dB)</b>
-90≤θ≤+90	1.86159	1.77157	1.65	0.77	2.17
-30≤θ≤+30	1.50029	1.79233	1.03	0.77	1.65
-90≤θ<-30 and +30<θ≤+90	2.05353	1.75838	1.785	0.76	2.5
<b>Fig.7b)</b>					
-90≤θ≤+90	3.29388	2.79373	2.92	0.88	5.1
-30≤θ≤+30	1.25118	1.30449	0.88	0.05	2.3
-90≤θ<-30 and +30<θ≤+90	4.37906	2.77541	4.365	1.63	6.65